

Band edge states of the $\langle n \rangle = 0$ gap of Fibonacci photonic lattices

A. Bruno-Alfonso,¹ E. Reyes-Gómez,² S. B. Cavalcanti,^{3,4} and L. E. Oliveira^{4,5}

¹Faculdade de Ciências, UNESP-Universidade Estadual Paulista, 17033-360, Bauru, São Paulo, Brazil

²Instituto de Física, Universidad de Antioquia, AA 1226, Medellín, Colombia

³Instituto de Física, Universidade Federal de Alagoas, Maceió, Alagoas, 57072-970, Brazil

⁴Inmetro, Campus de Xerém, Duque de Caxias, Rio de Janeiro, 25250-020, Brazil

⁵Instituto de Física, Universidade Estadual de Campinas-UNICAMP, CP 6165, Campinas, São Paulo, 13083-970, Brazil

(Received 14 May 2008; published 4 September 2008)

The stationary and normally incident electromagnetic modes in Fibonacci lattices with generating layers of positive and negative indices of refraction are calculated by a transfer-matrix technique. It is shown that the condition for constructive interference of reflected waves is fulfilled when the ratio of optical paths in positive and negative media are given by the golden ratio. Furthermore, in the long-wavelength limit, it is demonstrated that the edges of the $\langle n \rangle = 0$ gap are the frequencies satisfying the conditions $\langle \epsilon \rangle = 0$ and $\langle \mu \rangle = 0$.

DOI: 10.1103/PhysRevA.78.035801

PACS number(s): 42.70.Qs, 42.70.Gi

Conventional band gap materials based on right-handed electromagnetism, i.e., materials in which the phase velocity points in the same direction as the group velocity, have been extensively studied. They exhibit a photonic band gap due to the constructive interference of multiple Bragg scattering and thus, a sensitive gap with respect to changes of the lattice parameter [1]. Recently, materials exhibiting simultaneously negative permittivity ϵ and negative permeability μ and, therefore, a negative index of refraction $n = \sqrt{\epsilon\mu}$, have drawn considerable attention. These have been referred to as metamaterials, or left-handed materials, once idealized by Veselago [2], who deduced that the propagation of electromagnetic radiation through such media should exhibit backward wave propagation and reversed refraction. Lately, materials with ϵ near zero have also received considerable attention for their unexpected behavior that permits the squeezing and tunneling of radiation [3].

Theoretical and experimental studies [4–7] on the propagation of light through one-dimensional (1D) periodic arrays of alternating layers of positive and negative materials have evidenced the existence of a band gap which is insensitive to lattice parameter changes in contrast with the behavior exhibited by Bragg gaps. The physical origin of such a gap in periodic arrangements stems from the fact that there is no net phase change during propagation in the sense that the phase delay experimented in the positive media is reversed in the negative one and, therefore, there is no net phase delay in one unitary cell. This leads to the condition $\langle n \rangle = 0$ (null average of the refractive index), which depends only on the ratio of the layer thicknesses [8,9]. There are cases where the $\langle n \rangle = 0$ gap is omnidirectional, but this is not a rule [6].

Recently, the $\langle n \rangle = 0$ gap of 1D periodic arrays of alternating layers of air and a negative dispersive medium with Drude-type behavior has been thoroughly studied [9–11]. It has been demonstrated both the robustness of the $\langle n \rangle = 0$ gap to changes in the unit-cell size, and the fact that, in the long-wavelength limit, the lower and higher gap edges satisfy the $\langle \epsilon \rangle = 0$ and $\langle \mu \rangle = 0$ conditions. Furthermore, Da *et al.* [12] have theoretically analyzed the influence of losses in Fibonacci lattices containing left-handed material and concluded it does not change the characteristic of omnidirectional reflection.

In this work we study the $\langle n \rangle = 0$ gap of a periodic structure where the unit cell is a Fibonacci chain of layers *A* and *B*. Hence, the quasiperiodic limit is essentially attained when the number of layers in the unit cell is sufficiently large. The condition for constructive interference of reflected waves, known in periodic systems to define Bragg mirrors, leads to $\langle n \rangle = 0$ for the zeroth-order gap. Furthermore, in the long-wavelength limit, the gap-edge frequencies are shown to correspond to null average values of the electric and magnetic response functions.

Let us begin by considering a periodic layered structure with interfaces normal to the *z* axis, where each unit cell is composed by layers *A* and *B*. The constituent materials in *A* and *B* are air and a dispersive metamaterial following the dispersion law used by Li *et al.* [4], respectively. A diagram of this structure is shown in Fig. 1. The width, electric permittivity, and magnetic permeability of the layer *A* (*B*) are *a* (*b*), ϵ_A (ϵ_B), and μ_A (μ_B), respectively. Figure 2 displays the ratio between the dispersion laws governing the electric and magnetic responses, as well as the index of refraction, of the materials *A* and *B*. The responses are plotted as functions of the frequency $\nu = \omega / (2\pi)$. The harmonic electromagnetic waves which propagate along the *z*-axis direction with the magnetic field along the *x*-axis direction are described by the fields

$$\vec{H}(z, t) = \hat{e}_x \psi(z) e^{-i\omega t}, \quad \vec{E}(z, t) = \hat{e}_y \frac{ic\varphi(z)}{\omega} e^{-i\omega t}, \quad (1)$$

where $\psi(z)$ and $\varphi(z) = \psi'(z) / \epsilon(z)$ satisfy

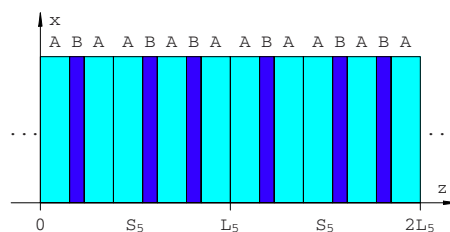


FIG. 1. (Color online) Photonic lattice whose unit cell is the Fibonacci chain $S_5 = ABAABABA$.

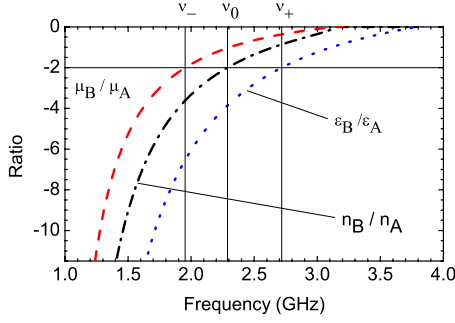


FIG. 2. (Color online) The ratio between the dispersion laws of materials A and B.

$$-\varphi'(z) = \omega^2 \mu(z) \psi(z) / c^2. \quad (2)$$

Moreover, both $\psi(z)$ and $\varphi(z)$ should be continuous across the interfaces. Let L be the size of the lattice unit cell. This means that $\epsilon(z+L) = \epsilon(z)$ and $\mu(z+L) = \mu(z)$. Due to the translational invariance of the lattice, the functions $\psi(z)$ may be labeled by the Bloch wave vector q , i.e., they satisfy the Bloch condition $\psi_q(z+L) = e^{iqL} \psi_q(z)$.

The Fibonacci chain of m th order is obtained according to the concatenation rule $S_m = S_{m-1} S_{m-2}$, with the first two chains as $S_0 = B$ and $S_1 = A$. For instance, the chain of fifth order is $S_5 = ABAABABA$, as shown in Fig. 1. This kind of structure has been theoretically [4,12] and experimentally [13] investigated. The number of layers in S_m is the Fibonacci number F_{m+1} , where $F_1 = 1$, $F_2 = 1$, and $F_m = F_{m-2} + F_{m-1}$. A very important property of the Fibonacci numbers involves the quotient $\tau_m = F_{m+1}/F_m$, with

$$\lim_{m \rightarrow \infty} \tau_m = \tau = (1 + \sqrt{5})/2. \quad (3)$$

The number of layers of type A (B) in S_m is F_m (F_{m-1}). Hence, the period of the lattice based on S_m is $L_m = F_m a + F_{m-1} b$. Furthermore, the optical path along the unit cell is $\delta_m = F_m a n_A + F_{m-1} b n_B$, and the Bragg condition for constructive interference of reflected waves is given by

$$\delta_m = \frac{N\pi c}{\omega}, \quad (4)$$

where $N=0$ for the zeroth-order gap, i.e., the $\langle n \rangle = 0$ gap, and $N = \pm 1, \pm 2, \pm 3, \dots$ for the so-called Bragg gaps. The averaged refractive index is defined by

$$\langle n \rangle_m = (F_m a n_A + F_{m-1} b n_B) / L_m, \quad (5)$$

and the $\langle n \rangle = 0$ gap occurs around the frequency satisfying the condition $\langle n \rangle_m = 0$, i.e.,

$$a n_A + b n_B / \tau_{m-1} = 0. \quad (6)$$

In this way, the frequency for the limiting condition in the case of large m is given when the optical paths in media A and B are in the golden ratio; that is,

$$\frac{b|n_B|}{a n_A} = \tau. \quad (7)$$

To deal with layered structures, one may use a transfer-

matrix approach. According to Eq. (2) and the continuity conditions at the interfaces, the functions $\psi_q(z)$ and $\varphi_q(z)$ may be determined from the initial values $\psi_q(z_0)$ and $\varphi_q(z_0)$. In fact, for the frequency ω we arrive at

$$\begin{pmatrix} \psi_q(z) \\ \varphi_q(z) \end{pmatrix} = T(\omega, z, z_0) \begin{pmatrix} \psi_q(z_0) \\ \varphi_q(z_0) \end{pmatrix}, \quad (8)$$

where $T(\omega, z, z_0)$ is the transfer matrix from z_0 to z . Taking the Bloch condition into account, one may connect the values of ψ_q and φ_q at $z=0$ and $z=L$, with L being the lattice period. Thus one obtains

$$\begin{pmatrix} \psi_q(L) \\ \varphi_q(L) \end{pmatrix} = M(\omega) \begin{pmatrix} \psi_q(0) \\ \varphi_q(0) \end{pmatrix} = e^{iqL} \begin{pmatrix} \psi_q(0) \\ \varphi_q(0) \end{pmatrix}, \quad (9)$$

where $M(\omega) = T(\omega, L, 0)$ is the transfer matrix from 0 to L , for the frequency ω . Therefore, the relation between ω and q is

$$\cos(qL) = R(\omega), \quad (10)$$

with $R(\omega)$ being the semitrace of $M(\omega)$. Moreover, the allowed (forbidden) frequencies are those satisfying $|R(\omega)| \leq 1$ ($|R(\omega)| > 1$).

Let us now consider the elementary unit cell of the lattice consisting of N homogeneous layers with refractive index n_l and thicknesses d_l , where $l=1, 2, \dots, N$. The left (right) interface of the first (last) layer will be at $z=0$ ($z=L$). Hence, the transfer matrix from the left to the right interface of the l th slab is

$$T_l(\omega) = \begin{pmatrix} \cos(q_l d_l) & \frac{\epsilon_l}{q_l} \sin(q_l d_l) \\ -\frac{q_l}{\epsilon_l} \sin(q_l d_l) & \cos(q_l d_l) \end{pmatrix}, \quad (11)$$

where $q_l = \omega n_l / c$. The matrix $M(\omega)$ is a product of the transfer matrices of the slabs, namely,

$$M(\omega) = T_N(\omega) \cdot \dots \cdot T_2(\omega) \cdot T_1(\omega). \quad (12)$$

For the Fibonacci lattice based on the chain S_m , the transfer matrix $M(\omega)$, the semitrace $R(\omega)$, and the period L , are labeled by the index m . However, instead of Eq. (12), it is better to use the recurrence relation

$$M_m(\omega) = M_{m-2}(\omega) M_{m-1}(\omega), \quad (13)$$

where $M_0(\omega)$ and $M_1(\omega)$ have the form in Eq. (11), with l being B and A, respectively. The semitrace obeys the recurrence relation

$$R_m(\omega) = 2R_{m-1}(\omega)R_{m-2}(\omega) - R_{m-3}(\omega). \quad (14)$$

Then, the semitrace $R_m(\omega)$ may be easily calculated from $R_0(\omega) = \cos(q_B b)$, $R_1(\omega) = \cos(q_A a)$, and

$$R_2(\omega) = \cos(q_A a) \cos(q_B b) - \frac{1}{2} \left(\frac{\epsilon_B q_A}{\epsilon_A q_B} + \frac{\epsilon_A q_B}{\epsilon_B q_A} \right) \sin(q_A a) \sin(q_B b). \quad (15)$$

In Fig. 3 the photonic spectrum is depicted for Fibonacci lattices with $a=4$ mm, $b=2$ mm, and $2 \leq m \leq 10$. The fre-

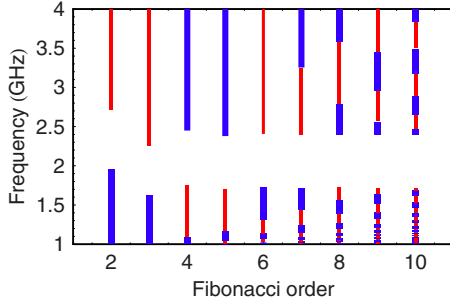


FIG. 3. (Color online) The photonic spectrum in Fibonacci lattices with $a=4$ mm and $b=2$ mm, as a function of the Fibonacci order. Consecutive bands are depicted as vertical-line segments of different widths.

quency range is chosen to clearly display the $\langle n \rangle = 0$ gap. The profile of this gap is shown in Fig. 4, as a function of the Fibonacci order, for three values of a with $a/b=2$. The best agreement with the long-wavelength approximation is obtained for the lattice with the thinner layers, i.e., for $a=4$ mm. Also, Fig. 4 suggests a convergence of the gap-edge frequencies, as the order m increases.

Let us now assume that $|q_A a| = \omega |n_A| a/c$ and $|q_B b| = \omega |n_B| b/c$ are much less than 1. In this regime $R_0(\omega) \approx R_1(\omega) \approx \dots \approx R_m(\omega) \approx 1$. Hence, there should be gap-edge frequencies satisfying $R_m(\omega) = 1$, which are associated with gaps at $q=0$. Approximate values of those frequencies may be obtained [10,11] by expanding $R_m(\omega)$ up to second order in $q_A a$ and $q_B b$. It may be shown that such an expansion reads,

$$R_m(\omega) \approx 1 - \omega^2 L_m^2 \langle \epsilon \rangle_m \langle \mu \rangle_m / (2c^2), \quad (16)$$

where the average permittivity and the average permeability are $\langle \epsilon \rangle_m = (F_m a \epsilon_A + F_{m-1} b \epsilon_B) / L_m$ and $\langle \mu \rangle_m = (F_m a \mu_A + F_{m-1} b \mu_B) / L_m$, respectively. The edge frequency corresponding to $\langle \epsilon \rangle = 0$ satisfies

$$a \epsilon_A + b \epsilon_B / \tau_{m-1} = 0, \quad (17)$$

and that for $\langle \mu \rangle = 0$ obeys

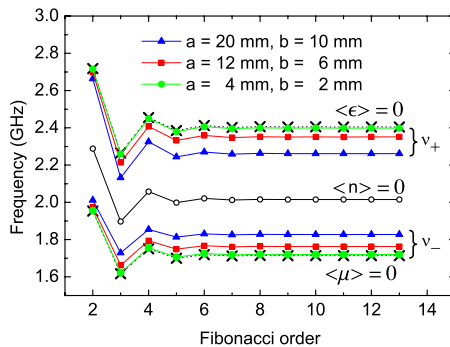


FIG. 4. (Color online) The $\langle n \rangle = 0$ -gap profile of Fibonacci lattices with $a/b=2$, as a function of the Fibonacci order m . The crosses are for the conditions $\langle \epsilon \rangle_m = 0$ and $\langle \mu \rangle_m = 0$.

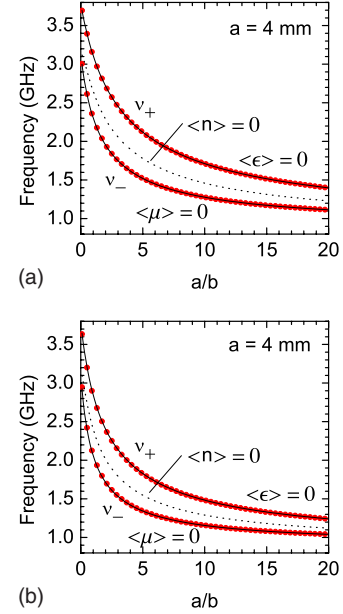


FIG. 5. (Color online) The $\langle n \rangle = 0$ -gap profile of Fibonacci lattices with $a=4$ mm, as a function of the ratio a/b . In (a) and (b), the Fibonacci order equals 2 and 11, respectively. The solid lines (dots) are for $\langle \epsilon \rangle_m = 0$ or $\langle \mu \rangle_m = 0$ [the solutions of $R_m(\omega) = 1$].

$$a \mu_A + b \mu_B / \tau_{m-1} = 0. \quad (18)$$

The limiting equations for large m are given by the following relations:

$$\frac{b |\epsilon_B|}{a \epsilon_A} = \tau \quad \text{and} \quad \frac{b |\mu_B|}{a \mu_A} = \tau, \quad (19)$$

which correspond to null averages of the response functions, i.e., $\langle \epsilon \rangle = 0$ and $\langle \mu \rangle = 0$, respectively. Figure 5 shows the gap edges, as functions of the ratio a/b with $a=4$ mm, for $m=2$ and $m=11$. Since the long-wavelength approximation applies, the frequencies satisfying Eqs. (17) and (18), displayed as solid lines in Fig. 5, are in excellent agreement with the numerical solutions of $R_m(\omega) = 1$ near the $\langle n \rangle = 0$ frequency.

To understand Eq. (16), it is useful to write $R_m(\omega) \approx 1 - \omega^2 g_m(\omega) / (2c^2)$. Since the second term in $g_m(\omega)$ is small, Eq. (14) leads to

$$g_m(\omega) = 2g_{m-1}(\omega) + 2g_{m-2}(\omega) - g_{m-3}(\omega). \quad (20)$$

We also have

$$\begin{aligned} g_0(\omega) &= n_B^2 b^2 = (b \epsilon_B)(b \mu_B) \\ &= (F_0 a \epsilon_A + F_{-1} b \epsilon_B)(F_0 a \mu_A + F_{-1} b \mu_B), \end{aligned} \quad (21)$$

$$\begin{aligned} g_1(\omega) &= n_A^2 a^2 = (a \epsilon_A)(a \mu_A) \\ &= (F_1 a \epsilon_A + F_0 b \epsilon_B)(F_1 a \mu_A + F_0 b \mu_B), \end{aligned} \quad (22)$$

and

$$\begin{aligned}
g_2(\omega) &= n_A^2 a^2 + n_B^2 b^2 + \left(\frac{\epsilon_B n_A}{\epsilon_A n_B} + \frac{\epsilon_A n_B}{\epsilon_B n_A} \right) n_A a n_B b \\
&= (a\epsilon_A + b\epsilon_B)(a\mu_A + b\mu_B) \\
&= (F_2 a \epsilon_A + F_1 b \epsilon_B)(F_2 a \mu_A + F_1 b \mu_B). \quad (23)
\end{aligned}$$

Then, using Eqs. (20)–(23), one arrives at

$$\begin{aligned}
g_m(\omega) &= (F_m a \epsilon_A + F_{m-1} b \epsilon_B)(F_m a \mu_A + F_{m-1} b \mu_B) \\
&= L_m^2 \langle \epsilon \rangle_m \langle \mu \rangle_m. \quad (24)
\end{aligned}$$

Note that $F_m F_{m-1}$ and F_m^2 satisfy the same recurrence relation as $g_m(\omega)$ does, namely, Eq. (20).

One may wonder whether the solutions of Eqs. (17) and (18) are the edges of a frequency gap. To answer this, we assume that in the frequency range of interest (i) $\epsilon_A > 0$ and $\mu_A > 0$, (ii) ϵ_B and μ_B may take any negative value, and (iii) ϵ_B and μ_B are monotonic functions of the frequency (see Fig. 2). This guarantees that Eqs. (17) and (18) have the unique solutions ν_ϵ^m and ν_μ^m , respectively. By using $g_m(\omega) = F_m^2 (a\epsilon_A + b\epsilon_B/\tau_{m-1})(a\mu_A + b\mu_B/\tau_{m-1})$, one may show that $R(\omega) > 1$ for $\nu_\epsilon^m < \nu < \nu_\mu^m$, which corresponds to a range of forbidden frequencies.

The lower and upper frequencies of the gap are denoted as ν_+^m and ν_-^m , respectively. To see whether ν_-^m is either ν_ϵ^m or ν_μ^m , it is useful to observe Fig. 2, where the ratios ϵ_B/ϵ_A and μ_B/μ_A are given as functions of the frequency. Since Eqs. (17) and (18) are equivalent to $\epsilon_B/\epsilon_A = -\tau_{m-1}a/b$ and $\mu_B/\mu_A = -\tau_{m-1}a/b$, respectively, the frequencies ν_ϵ^m and ν_μ^m may be graphically found by drawing a horizontal line at the height $-\tau_{m-1}a/b$ of the ratio. The case $a/b=2$ and $m=2$ is depicted in Fig. 2, where it is apparent that $\nu_-^m = \nu_\mu^m$ and $\nu_+^m = \nu_\epsilon^m$. It is important to note that the $\langle n \rangle = 0$ frequency is within the considered gap. This frequency is denoted as ν_0^m , and satisfies Eq. (6), i.e., $n_B/n_A = -\tau_{m-1}a/b$. The ratio n_B/n_A , as displayed in Fig. 2, is the geometric mean of the ratios

ϵ_B/ϵ_A and μ_B/μ_A . Therefore, it is clear that ν_0^m is between ν_μ^m and ν_ϵ^m .

We may wonder why, in the long-wavelength limit, the conditions $\langle \epsilon \rangle = 0$ and $\langle \mu \rangle = 0$ should apply at the edges of the $\langle n \rangle = 0$ gap. The reason is that for sufficiently low frequencies, the unit cell of the lattice behaves as an effective optical medium whose response is determined by the averaged values of permittivity and permeability. Considering the dispersion relations in Fig. 2, those averaged values are increasing functions of the frequency. From this, we obtain the following three cases: (i) if $\nu < \nu_\mu^m$, then $\langle \epsilon \rangle_m < 0$ and $\langle \mu \rangle_m < 0$, (ii) if $\nu_\mu^m < \nu < \nu_\epsilon^m$, then $\langle \epsilon \rangle_m < 0$ and $\langle \mu \rangle_m > 0$, and (iii) if $\nu > \nu_\epsilon^m$, then $\langle \epsilon \rangle_m > 0$ and $\langle \mu \rangle_m > 0$. Hence, in cases (i) and (iii) the wave propagates along the effective medium without absorption. This corresponds to the allowed frequencies. Instead, in case (ii) the refractive index of the effective medium is imaginary. Hence, the effective medium does not allow the propagation of the wave, and the corresponding frequency range should be a gap of the electromagnetic band structure.

Summing up, the propagation of light through a 1D lattice composed by layers of optical media *A* and *B*, of positive and negative refractive indices, arranged according to a concatenation rule of the Fibonacci type, has been studied. We have proven that a robust zeroth-order gap arises. Moreover, when the Fibonacci order is high, the gap occurs around the frequency for which the ratio of the optical paths is close to the golden ratio. In the long-wavelength limit, analytical expressions that define the gap edges around the zeroth-order gap were obtained, and the corresponding frequencies were shown to satisfy the $\langle \epsilon \rangle = 0$ and $\langle \mu \rangle = 0$ conditions.

The authors would like to thank the Brazilian Agencies CNPq, FAPESP, FAPERJ, MCT-Millennium Institute for Quantum Information, and MCT-Millennium Institute for Nanotechnology, as well as the Scientific Colombian Agency COLCIENCIAS, and CODI-University of Antioquia for partial financial support.

-
- [1] E. Istrate and E. H. Sargent, *Rev. Mod. Phys.* **78**, 455 (2006).
[2] V. G. Veselago, *Sov. Phys. Usp.* **10**, 509 (1968).
[3] B. Edwards, A. Alù, M. E. Young, M. Silveirinha, and N. Engheta, *Phys. Rev. Lett.* **100**, 033903 (2008).
[4] J. Li, L. Zhou, C. T. Chan, and P. Sheng, *Phys. Rev. Lett.* **90**, 083901 (2003).
[5] H. Jiang, H. Chen, H. Li, Y. Zhang, and S. Zhu, *Appl. Phys. Lett.* **83**, 5386 (2003).
[6] H. Daninthe, S. Foteinopoulou, and C. M. Soukoulis, *Photonics Nanostruct. Fundam. Appl.* **4**, 123 (2006).
[7] Y. Yuan, L. Ran, J. Huangfu, H. Chen, L. Shen, and J. A. Kong, *Opt. Express* **14**, 2220 (2006).
[8] S. B. Cavalcanti, M. de Dios-Leyva, E. Reyes-Gómez, and L. E. Oliveira, *Phys. Rev. B* **74**, 153102 (2006).
[9] S. B. Cavalcanti, M. de Dios-Leyva, E. Reyes-Gómez, and L. E. Oliveira, *Phys. Rev. E* **75**, 026607 (2007).
[10] L. Zhang, Y. Zhang, L. He, Z.-G. Wang, H. Li, and H. Chen, *J. Phys. D: Appl. Phys.* **40**, 2579 (2007).
[11] Y. Weng, Z.-G. Wang, and H. Chen, *Phys. Rev. E* **75**, 046601 (2007).
[12] H. X. Da, C. Xu, and Z. Li, *Phys. Lett. A* **345**, 459 (2005).
[13] L. Dal Negro, C. J. Oton, Z. Gaburro, L. Pavesi, P. Johnson, A. Lagendijk, R. Righini, M. Colocci, and D. S. Wiersma, *Phys. Rev. Lett.* **90**, 055501 (2003).